

# Analytical solutions for forced long waves on a sloping beach

By PHILIP L.-F. LIU<sup>1</sup>, PATRICK LYNETT<sup>1</sup>†  
AND COSTAS E. SYNOLAKIS<sup>2</sup>

<sup>1</sup>School of Civil and Environmental Engineering, Cornell University, Ithaca, NY 14853, USA

<sup>2</sup>School of Engineering, University of Southern California, Los Angeles, CA 90089-2531, USA

(Received 12 September 2002 and in revised form 22 November 2002)

We derive analytic solutions for the forced linear shallow water equation of the following form:

$$\frac{\partial^2 Y}{\partial t^2} - b \frac{\partial}{\partial x} \left( x \frac{\partial Y}{\partial x} \right) = \frac{\partial^2 f}{\partial t^2}$$

for  $x > 0$ , in which  $Y(x, t)$  denotes an unknown variable,  $f(x, t)$  a prescribed forcing function and  $b$  a positive constant. This equation has been used to describe landslide-generated tsunamis and also long waves induced by moving atmospheric pressure distributions. We discuss particular and general solutions. We then compare our results with numerical solutions of the same equation and with the corresponding solutions of the nonlinear depth-integrated equations and discuss them in terms of landslide-generated tsunamis.

## 1. Introduction

In considering tsunami generation by a moving slide on a uniform slope, Tuck & Hwang (1972) adopted the linear shallow water equation for a uniformly sloping beach in the following dimensionless form:

$$\frac{\partial^2 \zeta}{\partial t^2} - \frac{\tan \beta}{\mu} \frac{\partial}{\partial x} \left( x \frac{\partial \zeta}{\partial x} \right) = \frac{\partial^2 h_0}{\partial t^2}, \quad (1.1)$$

where  $z = \zeta(x, t)$  is the free surface elevation and  $z = -h(x, t)$  the sea floor. On a sloping beach  $h(x, t) = H(x) - h_0(x, t)$  with  $H(x) = x \tan \beta / \mu$ ;  $\tan \beta$  is the beach slope,  $h_0(x, t)$  is the time-dependent perturbation of the sea floor with respect to the uniformly sloping beach,  $\delta$  and  $L$  are the maximum vertical thickness of the sliding mass and its horizontal length respectively, and  $\mu = \delta / L$ . We have normalized the free surface displacement and water depth with  $\delta$ , and  $x$  with  $L$ , and  $t$ , as expected, with  $\sqrt{\delta / g} / \mu$ . Here, we will focus on thin slides where  $\mu = \delta / L \ll 1$ . Since the shallow water assumption requires that  $\tan \beta \ll 1$ , then  $\tan \beta / \mu \sim O(1)$ .

Greenspan (1956) has also derived an equation similar to (1.1) for long waves generated by moving atmospheric pressure distributions. Following Greenspan (1956), we can define a dimensionless velocity potential  $\phi$  so that its time derivative becomes

$$\phi_t = P_a(x, t) - \zeta, \quad (1.2)$$

† Present address: Department of Civil Engineering, Texas A&M University, College Station, TX 77843-3136, USA.

in which  $P_a$  denotes the dimensionless moving atmospheric pressure distribution. Once again, the free surface displacement has been scaled by  $\delta = P_0/\rho g$ , where  $\rho$  is the density of water and  $P_0$  the characteristic atmospheric pressure. In this problem, the horizontal and the vertical length scales are the same, i.e.  $\delta \sim L$  and  $\mu = 1$ . The governing equation for  $\phi_t$  over a constant sloping beach can be written in the dimensionless form

$$\frac{\partial^2 \phi_t}{\partial t^2} - \tan \beta \frac{\partial}{\partial x} \left( x \frac{\partial \phi_t}{\partial x} \right) = \frac{\partial^2 P_a}{\partial t^2}, \quad (1.3)$$

Once the atmospheric pressure is prescribed,  $\phi_t$  as well as the free surface displacement  $\zeta$  can be calculated from the above equations.

Since (1.1) and (1.3) are of the same form, here we focus only on the former in the context of landslide-generated tsunamis. Tuck & Hwang (1972) have shown that (1.1) can be solved by elementary Laplace and Hankel transformations. They presented results for several impulsive and transient beach floor movements. In the case of transient sea floor motion, they assumed that while the amplitude of the slide changes in time, the shape of the slide always remains the same, decaying exponentially in the offshore direction with the same decay rate. Here, we shall first present briefly a new solution of the forced shallow water wave equation, in which the slide is accelerating with a constant acceleration. For this type of slide motion, the particular solution of equation (1.1), can be obtained exactly. Specific results are obtained for slides with a Gaussian profile. To ensure that the analytical solution is derived correctly, it is verified with the direct numerical solutions solving the same equation (1.1). Then, the limitations of the governing equation (1.1) are discussed by comparing the analytical solutions with results obtained from numerical solutions of the nonlinear shallow water equations.

Finally we note that analytical solutions for the one-dimensional constant-depth forced equation have been presented by Tinti, Bortolucci & Chlavettieri (2001) and Okal & Synolakis (2003). Two-dimensional solutions in integral form based on Laplace's equations have been presented by Pelinofsky & Poplavsky (1996) and Ward (2001). Other semi-analytical and empirical results are also discussed in Synolakis (2002).

## 2. The analytical solution

### 2.1. Derivation

To find the analytical solution for (1.1), we make the following substitution:

$$\xi = 2\sqrt{\frac{\mu x}{\tan \beta}}, \quad (2.1)$$

and apply the Hankel transform defined as

$$\mathcal{H}(\rho, t) = \int_0^\infty \xi J_0(\rho \xi) \zeta(\xi, t) d\xi,$$

where  $J_0$  is the Bessel function of the first kind of order zero. Equation (1.1) becomes

$$\frac{\partial^2 \mathcal{H}}{\partial t^2} + \rho^2 \mathcal{H}(\rho, t) = \frac{\partial^2 \mathcal{H}_0}{\partial t^2}, \quad (2.2)$$

where  $\mathcal{H}_0(\rho, t)$  is the Hankel transform of  $h_0(\xi, t)$ , i.e. of the sea-floor deformation. Now consider a periodic ground movement, with frequency  $\omega$ , of the form

$$h_0(\xi, t) = e^{i\omega(\xi-t)}, \tag{2.3}$$

i.e. when the acceleration of the sea-floor movement is exactly equal to  $g \tan \beta/2$ , the velocity is  $\sqrt{gh}$ . After some algebra, and when  $\omega/\rho < 1$  and  $\omega, \rho > 0$ , the solution of the transformed equation (2.2) can be written as

$$\mathcal{H}(\rho, t) = \frac{i\omega^3 e^{-i\omega t}}{(\rho^2 - \omega^2)^{5/2}}. \tag{2.4}$$

Inverting the transform when  $\omega/\xi < 1$  and  $\omega, \xi > 0$ , we obtain

$$\zeta(\xi, t) = \frac{1}{3}(1 - i\xi\omega)e^{i\omega(\xi-t)}, \tag{2.5}$$

implying that a particular solution for a motion  $h_0(\xi - t)$  is given by

$$\zeta_p(\xi, t) = \frac{1}{3} \left( h_0 - \xi \frac{\partial h_0}{\partial \xi} \right). \tag{2.6}$$

Thus, the particular solution is determined exactly for a specified sea-floor movement  $h_0(\xi - t)$ .

The general solution of the forced equation (1.1) with a bottom perturbation  $h_0(\xi - t)$  is a combination of the particular solution (2.6) and the solution of the homogenous equation. The homogenous solution can be expressed as

$$\zeta_h(\xi, t) = \int_0^\infty \omega a(\omega) J_0(\omega\xi) \cos(\omega t) d\omega + \int_0^\infty \omega b(\omega) J_0(\omega\xi) \sin(\omega t) d\omega, \tag{2.7}$$

where  $a(\omega)$  and  $b(\omega)$  are to be determined by the initial conditions. At  $t = 0$ , the sum of the particular solution (2.6) and the homogenous solution, (2.7), is zero, corresponding to an initially unperturbed water surface. This allows the determination of  $a(\omega)$ . On the other hand,  $b(\omega)$  can be determined by requiring  $\zeta_t = h_0$ , at  $t = 0$ , i.e. velocity is zero everywhere at  $t = 0$ . Thus, we find

$$a(\omega) = -\frac{1}{3} \int_0^\infty \xi J_0(\omega\xi) \left( h_0 - \xi \frac{\partial h_0}{\partial \xi} \right)_{t=0} d\xi, \tag{2.8}$$

$$\omega b(\omega) = \frac{1}{3} \int_0^\infty \xi J_0(\omega\xi) \left( 2 \frac{\partial h_0}{\partial t} + \xi \frac{\partial^2 h_0}{\partial \xi \partial t} \right)_{t=0} d\xi. \tag{2.9}$$

The analytical solution is completed by substituting (2.8) and (2.9) into the homogenous solution, (2.7) and then adding the resulting homogenous solution to the particular solution (2.6).

Explicit expressions for  $a(\omega)$  and  $b(\omega)$  are possible for a translating Gaussian sea-floor movement, i.e.  $h_0(\xi, t) = \exp(-(\xi - t)^2)$ . From (2.8) and (2.9), we obtain

$$a(\omega) = -\frac{1}{3} \int_0^\infty \xi J_0(\omega\xi) (1 + 2\xi^2) e^{-\xi^2} d\xi = -\frac{1}{12} (6 - \omega^2) e^{-\omega^2/4}, \tag{2.10}$$

$$\begin{aligned} \omega b(\omega) &= \frac{2}{3} \int_0^\infty \xi^2 J_0(\omega\xi) (3 - 2\xi^2) e^{-\xi^2} d\xi \\ &= -\frac{\sqrt{\pi}}{48} \omega^2 e^{-\omega^2/8} [(\omega^2 - 6)I_0(\omega^2/8) - (\omega^2 - 2)I_1(\omega^2/8)], \end{aligned} \tag{2.11}$$

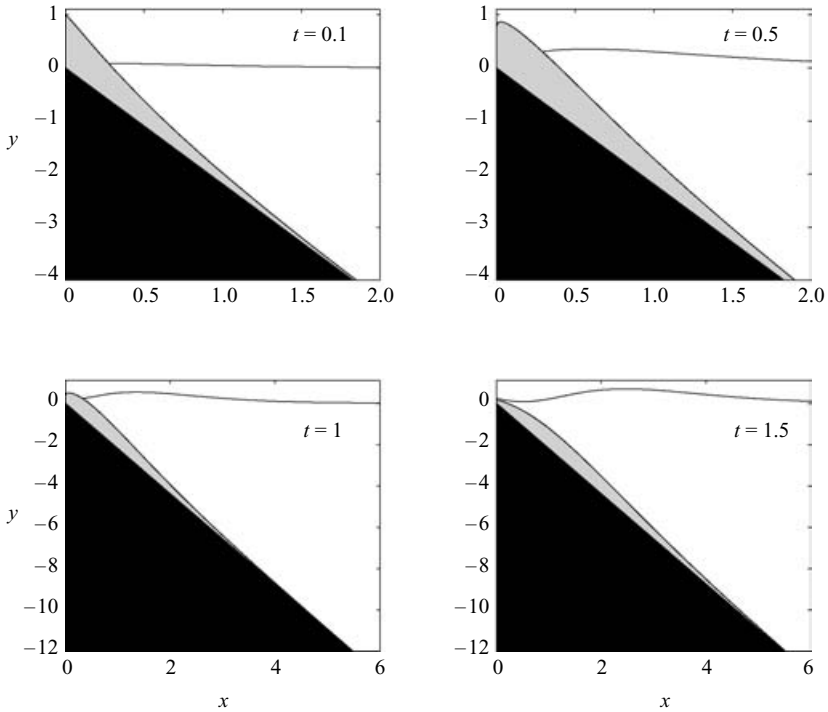


FIGURE 1. Spatial snapshots of the analytical solution at four different times for a beach slope,  $\beta = 5^\circ$ , and landslide aspect ratio,  $\mu = 0.05$  (i.e.  $\tan \beta/\mu = 1.75$ ). The slide mass is indicated by the light shaded area, the solid beach slope by the black region, and  $\zeta$  by the solid line.

in which  $I_0$  and  $I_1$  are modified Bessel functions of the first kind of order zero and one, respectively. Therefore, the homogenous solution is given by

$$\begin{aligned} \zeta_h(\xi, t) = & -\frac{1}{12} \int_0^\infty \omega(6 - \omega^2) J_0(\omega\xi) e^{-\omega^2/4} \cos(\omega t) d\omega \\ & - \frac{\sqrt{\pi}}{48} \int_0^\infty \omega^2 e^{-\omega^2/8} [(\omega^2 - 6) J_0(\omega^2/8) - (\omega^2 - 2) I_1(\omega^2/8)] J_0(\omega\xi) \sin(\omega t) d\omega, \end{aligned} \tag{2.12}$$

and the particular solution becomes

$$\zeta_p(\xi, t) = \frac{1}{3} [1 + 2\xi(\xi - t)] e^{(\xi-t)^2}. \tag{2.13}$$

Of course, the complete solution is

$$\zeta(\xi, t) = \zeta_p(\xi, t) + \zeta_h(\xi, t). \tag{2.14}$$

### 2.2. Discussion of the analytical solution

The integrals in (2.12) can be integrated numerically to find  $\zeta$ . In figure 1 snapshots of the solution for  $\zeta$  at four different times for a beach slope,  $\beta = 5^\circ$ , and landslide aspect ratio,  $\mu = 0.05$ , are shown (i.e.  $\tan \beta/\mu = 1.75$ ). The slide mass is indicated by the light shaded area, and  $\zeta$  by the solid line. The sliding mass, partially submerged at first, pushes water away from the beach as it begins to slide down the slope.

A leading elevation  $N$ -wave forms, propagating in the offshore direction, as the slide becomes completely submerged.

As a primary, fundamental check of the analytical solution, (1.1) is solved directly numerically. Following Kirby, Dalrymple & Liu (1981), the transformation  $Z = x\zeta$  is employed, yielding the transformed linear shallow water equation:

$$Z_{tt} - \frac{\tan \beta}{\mu} \left( xZ_{xx} - Z_x + \frac{Z}{x} \right) = xh_{0,t}. \tag{2.15}$$

The above equation has the advantage of simple and precise spatial boundary conditions; namely,  $Z(x=0, t) = 0$  and  $Z(x=\infty, t) = 0$ . The latter assumes that  $1/\zeta$  goes to zero faster than  $x$  goes to infinity. With the initial conditions  $Z(x, t=0) = 0$  and  $Z_t(x, t=0) = xh_{0,t}$ , and a simple finite-difference time marching scheme, it is readily shown that the numerical and analytical solutions agree almost exactly. This exercise has served its purpose: the analytical solution is a complete and correct solution.

Note that the solution outlined in the previous section exists for  $x > 0$ , regardless of whether  $\zeta + h < 0$ , as can be the case near  $\xi = 0$  at the early times. This is because in (1.1) the moving slide mass is represented only by a forcing term in the field equation, and not by the evolving change in the water depth profile. This is a direct consequence of dropping  $(h_0\zeta_x)_x$  during depth averaging, equivalent to considering the net horizontal mass flux caused directly by the slide motion,  $(uh_0)_x$  or  $(h_0\zeta_x)_x$ , as a higher-order term. The validity of this assumption will be examined in the next section. We note here that if the solutions obtained in the previous section are applied to atmospheric-pressure-generated waves, (1.3), this simplification is not necessary.

### 3. Comparison with nonlinear numerical models

#### 3.1. Nonlinear shallow water equations

The nonlinear shallow water (NLSW) equations are

$$\frac{\partial}{\partial t}(\zeta - h_0) + \frac{\partial}{\partial x} \left[ \left( \frac{\tan \beta}{\mu} x - h_0 + \zeta \right) u \right] = 0, \quad \frac{\partial u}{\partial t} + u \frac{\partial u}{\partial x} + \frac{\partial \zeta}{\partial x} = 0, \tag{3.1}$$

where  $u$  is the depth-averaged velocity. Note that the above equations include the forcing due to sea-floor movement,  $(uh_0)_x$ .

The numerical model employed here to solve the NLSW equations is a high-order finite-difference scheme, described in detail in Lynett & Liu (2002). The model utilizes a moving boundary algorithm which has been shown to be accurate for a variety of problems (Lynett, Wu & Liu 2002). This moving boundary scheme tracks the real shoreline, i.e. the location where  $\zeta + h = 0$ , and also locations where  $\zeta + h < 0$  cannot exist. This is noted again because, as mentioned earlier, this is not the case with the analytical solution as an analytic function does not end abruptly at the shoreline. It is expected that this discrepancy in the shoreline condition between the analytical and numerical models should lead to different results, with the numerical approach representing a better approximation to the real shoreline.

#### 3.2. Numerical comparisons with analytical solutions

First, the linear form of (3.1) is solved using the numerical procedure described above. This model considers  $(\zeta u)_x$  and  $uu_x$  as being higher order, and they are not calculated during the numerical integration. The linear numerical results and the

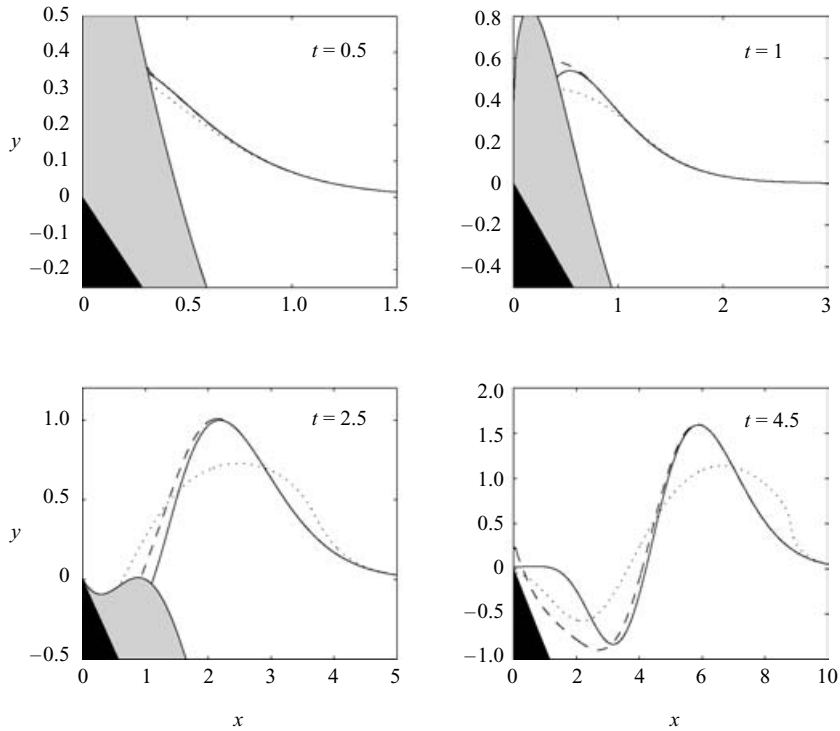


FIGURE 2. Spatial snapshots of the analytical (solid line), LSW with 'real' shoreline (dashed line), and NLSW solution (dotted line) at four different times for a beach slope,  $\beta = 5^\circ$ , and  $\mu = 0.10$  ( $\tan \beta/\mu = 0.87$ ). The slide mass is indicated by the light shaded area, and the solid beach slope by the black region.

analytical solution are shown in figures 2 and 3. The corresponding values for the dimensionless parameter  $\tan \beta/\mu$  are 0.87 and 3.5, respectively. In both cases, at small times ( $t < 1$ ), the numerical and analytical results match well up to the 'real' shoreline, indicating that the moving shoreline boundary and slide-related depth effects, i.e.  $(h_0 \zeta_x)_x$ , are not yet important. As time progresses, differences between the solutions at the real shoreline ( $\zeta + h = 0$ ) grow, and the solutions do not agree to a high degree near the shoreline. However, at large times the offshore wave height and shape agrees very well. These results show the minor deficiency of the shoreline condition used in the analytical solution due to the approximation  $H \approx h$ . It is also important to recognize that the agreement between the analytical solutions and the numerical linear shallow water (LSW) solutions is better for larger  $\tan \beta/\mu$  values.

Figures 2 and 3 also show NLSW results. As with the LSW comparison, at early times the numerical and analytical results match rather well. Up to this time, the accumulating effects of nonlinearity are small relative to the linear driving force of the physical problem. For later times, this is no longer the case. For  $\tan \beta/\mu = 0.87$  (figure 2) the generated wave is propagating in a water depth of the same order as its amplitude, and nonlinear propagation effects become important. At  $t = 4.5$ , a classic nonlinear vs. linear comparison, where nonlinearity is important, is evident. The nonlinear wave height is smaller, and the nonlinear crest is travelling at a faster speed. On the other hand, for  $\tan \beta/\mu = 3.5$  (figure 3) both the analytic solution and LSW numerical agree very closely with the NLSW numerical results. From these

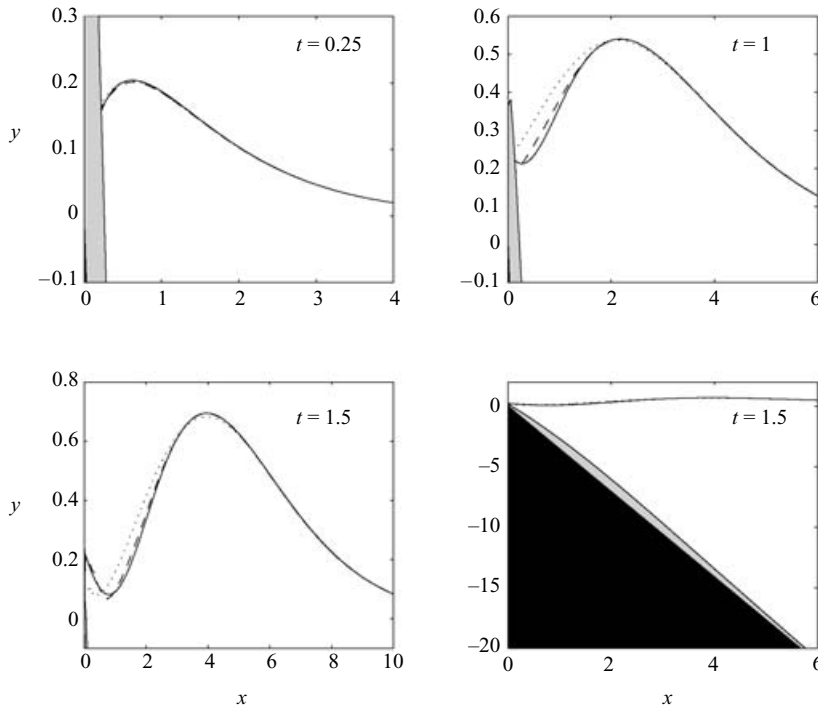


FIGURE 3. Spatial snapshots of the analytical (solid line), LSW with ‘real’ shoreline (dashed line), and NLSW solution (dotted line) at three different times for a beach slope,  $\beta = 10^\circ$ , and  $\mu = 0.05$  ( $\tan \beta/\mu = 3.5$ ). The slide mass is indicated by the light shaded area, and the solid beach slope by the black region. In the lower right panel, the water depth and landslide profile is shown at  $t = 1.5$ , the same time as shown in the lower left plot.

comparisons, we can conclude that the effects of nonlinearity, the ‘real’ shoreline boundary condition, and the approximation of  $H \approx h$  decrease with increasing  $\tan \beta/\mu$  values. As the NLSW model is theoretically applicable for mild slopes only, it is therefore expected that the analytic solution will be accurate only for small  $\mu$ .

In an attempt to roughly determine when the analytical and NLSW solutions converge, a runup comparison is now presented. Figure 4 shows the maximum runup (free surface elevation at the shoreline) predicted by the analytical solution and the NLSW equation. Runup given by the analytical solution decreases linearly with increasing  $\log(\tan \beta/\mu)$ , until about  $\log(\tan \beta/\mu) \approx 0.44$ , where it flattens at a runup value  $\approx 0.27$ . It flattens because at this  $\log[\tan \beta/\mu]$  value, the maximum runup becomes the maximum free surface at  $x = 0$ , which in the analytic solution is invariant to  $\tan \beta/\mu$ . In other words, for large  $\tan \beta/\mu$ , the maximum runup occurs after the slide has become completely submerged. It is interesting to observe that all of the NLSW runups fall onto one curve which is a function of  $\tan \beta/\mu$ . This NLSW curve does not agree well with the analytic solution for small  $\tan \beta/\mu$  values, but does converge with the analytic solution for large  $\tan \beta/\mu$ .

Therefore, as was the conclusion when examining the spatial snapshots of figures 2 and 3, the analytical solution gives an accurate representation of the physics of the subaerial landslide problem for large  $\tan \beta/\mu$ . The runup comparisons show that the analytic solution will be correct for  $\tan \beta/\mu > 10$ , although it was also shown that a high degree of agreement in the spatial profiles was found for  $\tan \beta/\mu = 3.5$ . For

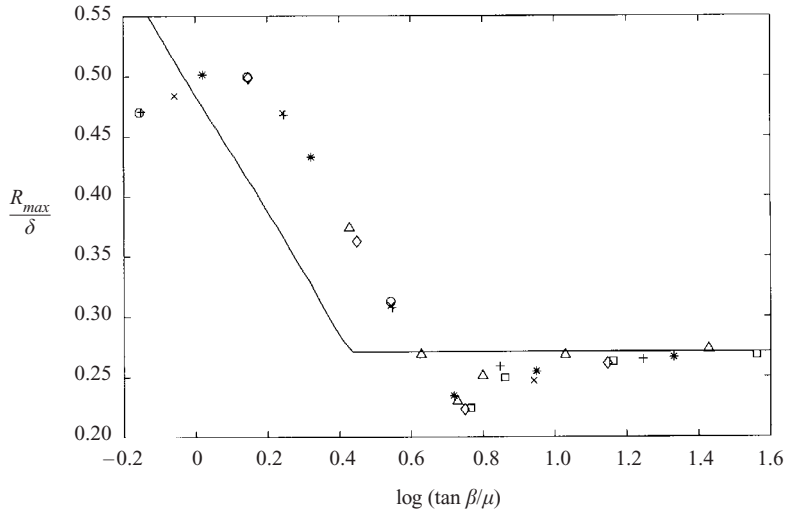


FIGURE 4. Maximum runup as a function of  $\log(\tan \beta/\mu)$ . The analytical solutions are shown by the solid line, and the various symbols are from NLSW simulations, corresponding to different slopes ranging from  $2^\circ$  to  $20^\circ$ .

$\tan \beta/\mu$  less than 1, it is expected that nonlinearity will play a leading role in the evolution of the generated wave. Nonetheless, the analytical solution produces estimates differing by less than 10% up to about  $\log(\tan \beta/\mu) \sim 0.5$ , another manifestation of the counterintuitive predictive prowess of linear theory in calculating wave runup on sloping beaches.

#### 4. Concluding remarks

We derive analytical solutions for waves generated by a moving block landslide down a sloping beach. Our derivation of linear wave generation and propagation represents a simplified solution to a very complex and vexing problem. The analyses imply that the analytical solutions capture the physics of the subaerial landslide problem for thin slides, while missing the nonlinear propagation aspects of the waves generated by thick slides. Regardless of an accurate characterization of the problem, the analytical solution is an excellent benchmark simulation tool for wave-generating, moving-boundary schemes in numerical models. While large-scale experiments are currently under way to generate comprehensive data sets for model validation (Synolakis & Raichlen 2002), analytical solutions are invaluable in helping validate computational techniques and in establishing relevant dimensionless scales such as  $\tan \beta/\mu$ .

We would like to thank Dr Cliff Astill, director of Geo-Hazard program at the National Science Foundation, for his continuous support.

#### REFERENCES

- GREENSPAN, H. P. 1956 The generation of edge waves by moving pressure distributions. *J. Fluid Mech.* **1**, 574–590.
- KIRBY, J. T., DALRYMPLE, R. A. & LIU, P. L.-F. 1981 Modification of edge waves by barred-beach topography. *Coastal Engng* **5**, 35–49.



- LYNETT, P. & LIU, P. L.-F. 2002 A numerical study of submarine landslide generated waves and runup. *Proc. R. Soc. Lond. A* **458**, 2885–2910.
- LYNETT, P., WU, T.-R. & LIU, P. L.-F. 2002 Modeling wave runup with depth-integrated equations. *Coastal Engng* **46**, 89–107.
- OKAL, E. O. & SYNOLAKIS, C. E. 2003 Theoretical comparisons of tsunamis from dislocations and slides. *Pure Appl. Geophys.* in press.
- PELINOFSKY, E. & POPLAVSKY, A. 1996 Simplified model of tsunami generation by submarine landslide. *Phys. Chem. Earth* **21** (12), 13–17.
- SYNOLAKIS, C. E. 2002 Tsunami and Seiche. In *Earthquake Engineering Handbook* (ed. W.-F. Chen & C. Scawthorn), pp. 9.1–9.90. CRC Press.
- SYNOLAKIS, C. E. & RAICHLIN, F. 2002 Wave and run-up generated by a three-dimensional sliding mass. *28th Intl Conf. Coastal Engng*, Abstracts, Paper 299.
- TINTI, S., BORTOLUCCI, E. & CHLAVETTIERI, C. 2001 Tsunami excitation by submarine slides in shallow-water approximation. *Pure Appl. Geophys.* **158**, 759–797.
- TUCK, E. O. & HWANG, L. S. 1972 Long wave generation on a sloping beach. *J. Fluid Mech.* **51**, 449–461.
- WARD, S. N. 2001 Landslide tsunami. *J. Geophys. Res.* **106**, 11201–11215.